Anomalous Collisions of Elastic Vector Solitons in Mechanical Metamaterials

Bolei Deng, Vincent Tournat, Pai Wang, and Katia Bertoldi

Phys. Rev. Lett. **122**, 044101 — Published 1 February 2019
DOI: 10.1103/PhysRevLett.122.044101

Anomalous Collisions of Elastic Vector Solitons in Mechanical Metamaterials

Bolei Deng,[1] Vincent Tournat,[2,3] Pai Wang,[1,4] and Katia Bertoldi[3,5]

[1]*Harvard John A. Paulson School of Engineering and Applied Sciences, Harvard University, Cambridge, MA 02138*
[2]*LAUM, CNRS, Université du Maine, Av. O. Messiaen, 72085 Le Mans, France*
[3]*Harvard John A. Paulson School of Engineering and Applied Science, Harvard University, Cambridge, MA 02138*
[4]*The Concord Consortium, Concord, MA 01742, USA*
[5]*Kavli Institute, Harvard University, Cambridge, MA 02138**

(Dated: January 2, 2019)

We investigate via a combination of experiments and numerical analyses the collision of elastic vector solitons in a chain of rigid units connected by flexible hinges. Due to the vectorial nature of these solitons, very unusual behaviors are observed: while, as expected, the solitons emerge unaltered from the collision if they excite rotations of the same direction, they do not penetrate each other and instead repel one another if they induce rotations of opposite direction. Our analysis reveals that such anomalous collisions are a consequence of the large-amplitude characteristics of the solitons, which locally modify the properties of the underlying media. Specifically, their large rotations create a significant barrier for pulses that excite rotations of opposite direction and this may block their propagation. Our findings provide new insights into the collision dynamics of elastic solitary waves. Furthermore, the observed anomalous collisions pave new ways towards the advanced control of large amplitude mechanical pulses, as they provide opportunities to remotely detect, change or destruct high-amplitude signals and impacts.

Collisions are one of the most fascinating features of solitary waves and have been investigated in many areas of science, including optics [1, 2], electronics [3], plasmonics [4, 5], quantum mechanics [6], general relativity [7] and mechanics [8–10]. Typically, the solitons are found to emerge from the collision unchanged (except for a phase shift [3, 5, 6] or the formation of small secondary waves [8–10]), as if there had been no interaction at all. This remarkable behavior led Zabusky and Kruskal [11] to coin the name 'soliton' (after photon, proton, etc.), to emphasize the particle-like character of these wave pulses [12]. While passing through one another without change of shape, amplitude, or speed is one of the defining properties of solitons [6], few exceptions have been found for solitary waves that propagate in systems that are either damped or not fully integrable. Specifically, the collision between a kink and its anti-kink pair has been shown to lead to a trapped breather in the integrable sine-Gordon system with damping [13], to a localized bound pair in the non-integrable ϕ^4 model [14] and to different types of kinks in the non-integrable double sine-Gordon model [13].

In this study, we focus on a mechanical metamaterial based on rotating rigid units [15–18] and use a combination of experiments and numerical analyses to study the collisions between two supported elastic vector solitons. Surprisingly, despite of the fact that the propagation of a single soliton is accurately captured by the completely integrable modified Korteweg-de Vries (mKdV) equation, not all solitary waves emerge unaltered from the collisions. If the propagating solitons induce rotations of opposite direction at a given unit in the system, they repel each other upon collision. We show that this highly unusual behavior is closely related to the vectorial nature of the supported solitons, which in turn leads to the formation of amplitude gaps - ranges in amplitude where elastic soliton propagation is forbidden. The large rotations induced by a soliton create a barrier for pulses with rotational component of opposite sign that blocks their propagation. Our study provides new insights into the collision dynamics of elastic solitary waves and reveals that in vector solitons the coupling between the different components can lead to completely unexplored and new phenomena.

Our mechanical metamaterial consists of a chain of N pairs of rigid crosses connected by thin and flexible hinges (see Fig. 1A). It has been recently shown that the propagation of a single soliton in such system is accurately described by a nonlinear Klein-Gordon equation [16], which can be rewritten in the form of the completely integrable mKdV equation [19]. The solution of such equation indicates that the considered metamaterial supports the propagation of elastic vector solitons that induce simultaneous longitudinal displacement u_i and rotation θ_i at the i-th pair of crosses, with all neighboring units rotating in opposite directions (see Fig. 1A). Specifically, u_i and θ_i are defined by [16] (see Supplementary Materials)

$$u_i\left(t\right) = \frac{aA^2W}{2(1-c^2/c_0^2)}\left[1-\tanh\left(\frac{ia-ct}{W}\right)\right] \qquad (1)$$

and

$$\theta_i\left(t\right) = A\,\mathrm{sech}\left(\frac{ia-ct}{W}\right), \qquad (2)$$

where a denotes the center-to-center distance between neighboring units and c_0 is the velocity of the supported linear longitudinal waves in the long wavelength limit. Moreover, A, c and W denote the amplitude, speed and

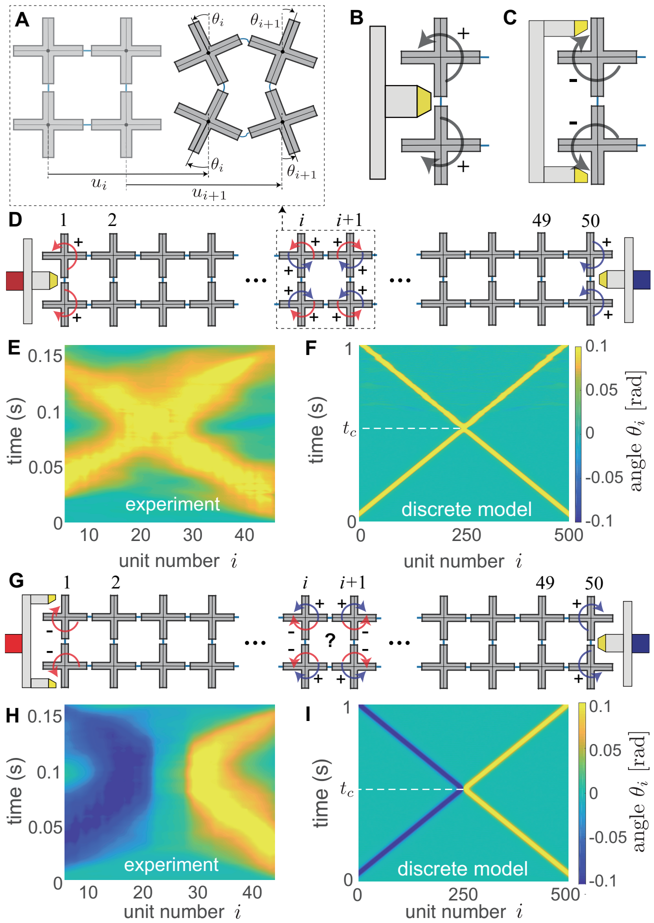

FIG. 1. (A) Schematic of the system. (B)-(C) Schematics of the impactors used to excite (B) positive and (C) negative rotations. (D) Schematic of our first experiment. (E)-(F) Rotation of the pairs of crosses during the propagation of the pulses, as recorded during our first test in (E) experiments and (F) numerical simulations. (G) Schematic of our second experiment. (H)-(I) Rotation of the pairs of crosses during the propagation of the pulses, as recorded during our second test in (H) experiments and (I) numerical simulations.

width of the pulses, with speed and width that can be expressed in terms of amplitude as

$$c = \pm c_0 \sqrt{\frac{6K_\theta}{A^2 + 6K_\theta}}, \tag{3}$$

and

$$W = \frac{a}{\alpha}\sqrt{\frac{\alpha^2(K_s - K_\theta) - 6K_\theta/(A^2+6K_\theta)}{6K_\theta}}. \tag{4}$$

where α represents the normalized mass, and K_s and K_θ are the normalized shear and bending stiffnesses of the hinges. At this point it is important to note that the propagation of the vector solitons defined by Eqs. (1) and (2) requires a strong coupling among their two components u_i and θ_i [20]. Since in our system such strong coupling is activated only for large enough rotations, vector solitons with

$$|A| < \sqrt{\frac{6K_s}{\alpha^2(K_s - K_\theta)} - 6K_\theta} \tag{5}$$

cannot propagate, resulting in the emergence of amplitude gaps [16]. While Eq. (5) fully defines the amplitude gap for a chain in which all hinges are aligned, pre-rotations of the crosses significantly increase the magnitude of the lower threshold, as they make the propagation of solitons that induce energetically unfavourable rotation more difficult [16]. Notably, our analysis will reveal that such pre-rotation effect on the amplitude gap plays a central role in defining the collision dynamics.

To investigate the collision of solitons in our system, we test a structure comprising $N = 50$ pairs of crosses made with LEGO bricks and connected via polyester plastic sheets. To initiate elastic vector solitons, we use two impactors that induce simultaneous rotation and displacement of the crosses at both ends of the sample (see Figs. 1B and C, and Supplementary Materials). We control the amplitude of the pulses by varying the maximum distance traveled by the impactors. As for the direction of rotation imposed to the first and last pairs of crosses, we select it by using two different types of impactors. Specifically, since we define as positive a clockwise (counter-clockwise) rotation of the top unit in the even (odd) pairs, we use an impactor that hits the midpoint of the end pairs to excite positive θ_i (see Fig. 1B) and one that hits their external arms to excite negative θ_i (see Fig. 1C - note that the direction of rotations imposed by the impactors changes if the chain comprises an odd number of pairs, see Supplementary Materials). In addition to the experiments, we also simulate the response of a chain with $N = 500$ pairs of crosses (to eliminate possible boundary effects) by numerically integrating the $2N$ ordinary differential equations with parameters $\alpha = 1.8$, $K_s = 0.02$ and $K_\theta = 1.5 \times 10^{-4}$ [16].

In Figs. 1E-F and H-I, we present experimental and numerical results for two sets of input signals applied to the left and right ends of the chain. First, the impactors excite solitons with amplitude $A_{\text{left}} = A_{10} = 0.2$ and $A_{\text{right}} = A_{N-10} = 0.2$ (A_i being the amplitude of θ_i before the collision). Both our experimental and numerical results indicate that the two pulses, which induce rotations with the same direction at any given unit in the chain (see Fig. 1D), penetrate each other without change of shape, amplitude or speed (see Fig. 1E and F and Supplementary Movie 1). As commonly observed when two solitons collide [3–10], only a slight time delay may be observed, confirming that our metamaterial can respond similarly to a fully integrable system such as a KdV system [13, 21]. Second, we apply $A_{\text{left}} = -0.2$ and $A_{\text{right}} = 0.2$ to excite two pulses that induce rotations of opposite sign at any given unit (see Fig. 1G).

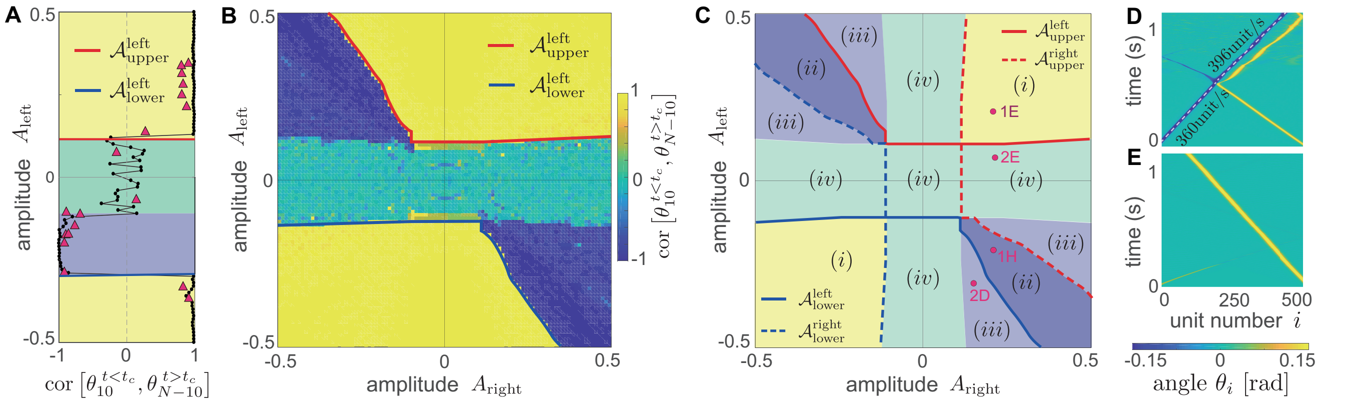

FIG. 2. (A) Cross-correlation between $\theta_{10}(t < t_c)$ and $\theta_{N-10}(t > t_c)$ as a function of A_{left} for $A_{\text{right}} = 0.2$. Triangular markers correspond to experimental data, while the black line is generated using numerical simulations. (B) Numerically obtained cross-correlation between $\theta_{10}(t < t_c)$ and $\theta_{N-10}(t > t_c)$ as a function of A_{left} and A_{right}. (C) Complete picture of the collision dynamic between the pulses supported by the system. (D)-(E) Rotations of the pairs of crosses during the propagation of the pulses as found in numerical simulations for (D) (A_{left}, A_{right}) = (-0.3,0.22) and (E) (0.08,0.3).

Surprisingly, we find that in this case the solitons do not penetrate each other and instead reflect one another (see Figs.1H and I and Supplementary Movie 1). This phenomenon is especially visible from the absence of rotations of the units in the center of the system. It is also important to note that, while in the experiments there is inevitably some dissipation due to both friction and viscous effects, in our numerical simulation we do not include any damping. As such, our results indicate that the observed anomalous collisions are not due to the presence of damping or boundary effects, and are rather a robust feature of the system.

To better understand how two colliding solitons interact in our system, we focus on the left-initiated pulse and systematically investigate how it is affected by the collision with the right-initiated one. To quantify such effect, we calculate the cross-correlation between $\theta_{10}(t < t_c)$ and $\theta_{N-10}(t > t_c)$ (t_c denoting the time at which the collision occurs) as a function of A_{left}, while keeping $A_{\text{right}} = 0.2$. As shown in Fig. 2A, we find that the response of the system is characterized by two distinct regions. For $A_{\text{left}} < \mathcal{A}^{\text{left}}_{\text{lower}} = -0.28$ and $A_{\text{left}} > \mathcal{A}^{\text{left}}_{\text{upper}} = 0.12$ the left-initiated elastic vector solitons propagate through the entire structure unaffected by the collision with the right-initiated pulses and the cross-correlation approaches unity. By contrast, for $\mathcal{A}^{\text{left}}_{\text{lower}} < A_{\text{left}} < \mathcal{A}^{\text{left}}_{\text{upper}}$ the left-initiated pulse does not reach the other end of the chain and the cross-correlation is $<< 1$. Focusing on this region of low cross-correlation, two recognizably different behaviors are observed. First, for $-0.12 < A_{\text{left}} < \mathcal{A}^{\text{left}}_{\text{upper}}$ the cross-correlation approaches zero, since the propagation of the left-initiated soliton is prevented by the amplitude gap of the chain defined by Eq. (5) (note that for this range of amplitudes no collision occurs, since the left-initiated soliton dies before reaching the right-initiated one). Second, for $\mathcal{A}^{\text{left}}_{\text{lower}} < A_{\text{left}} < -0.12$ the cross-correlation approaches -1. For this range of amplitudes a solitary wave that induces rotations with direction opposite from those excited by the left-initiated soliton is detected at the right end after collision - a clear signature of an anomalous collision dynamics that results in the (partial or total) reflection of the right-initiated soliton.

Next, we consider the effect on the collision of both A_{left} and A_{right}. The heat map shown in Fig. 2B confirms that, while typical collisions that do not alter the left-initiated soliton (resulting in a cross-correlation that approaches 1) occur when the two colliding solitons induce rotation of the same direction (i.e. $A_{\text{left}}\, A_{\text{right}} > 0$), anomalous collisions that change the left-initiated pulse (leading to a cross-correlation $\ll 1$) may also exist when two colliding solitons induce rotations of opposite direction (i.e. $A_{\text{left}}\, A_{\text{right}} < 0$). We then construct a plot analogous to that shown in Fig. 2B, but focused on the right-initiated pulses by considering the cross-correlation between $\theta_{N-10}(t < t_c)$ and $\theta_{10}(t > t_c)$ (see Fig. S7). By combining Fig. 2B with Fig. S7, we find that four different scenarios are possible upon collision (see Fig. 2C): (*i*) both solitons penetrate, as typical for collisions between solitons (see yellow area in Fig. 2C and Figs. 1D-E); (*ii*) both solitons are reflected - a clear signature of an anomalous collision (see dark blue area in Fig. 2C and Figs. 1G-H); (*iii*) one soliton is blocked and the other penetrates - again signature of an anomalous collision (see shallow blue area in Fig. 2C and Fig. 2D); (*iv*) one or no soliton travels through the system due to the existence of the amplitude gap, so that no collision occurs (see green area in Fig. 2C and Fig. 2E). Therefore, our numerical investigation describes quantitatively all possible two-solitons heads-on collisions and provides a complete picture of the collision dynamic between the pulses supported by the system.

The results of Figs. 1 and 2 reveal that our system supports anomalous collisions that alter the characteristics of the solitons. Such surprising phenomenon can be fully explained via the concept of amplitude gaps. The large rotations generated by a soliton effectively enlarge the amplitude gap for pulses that induce rotations of opposite sign, stopping their propagation when they come close enough. To demonstrate this important point, we freeze solitons of different amplitude $A_{\rm f}$ in the middle of the chain and numerically investigate their effect on the propagation of solitary waves initiated at the left end. Specifically, we consider a chain in which the i-th pair of crosses is rotated according to theoretical solution of soliton (see Fig. 3A and Supplementary Materials), excite pulses of different amplitude $A_{\rm left}$ at its left end and investigate the interaction between the left-initiated soliton and the frozen perturbation by looking at the cross-correlation between $\theta_{10}(t)$ and $\theta_{N-10}(t)$. The numerical results reported in Fig. 3B clearly indicate that there is a well-defined region in the $A_{\rm left}$-$A_{\rm f}$ space resulting in left-initiated solitons that do not reach the right end of the chain (note that in this region the cross-correlation is close to zero everywhere, as there is no propagating right-initiated pulse that can be reflected). Notably, we also

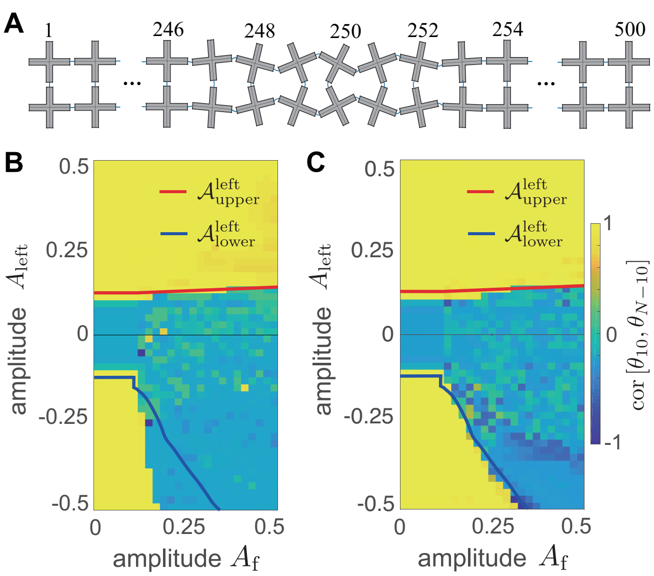

FIG. 3. (A) A $N = 500$ chain with a frozen soliton placed in the middle of it. (B)-(C) Numerically obtained cross-correlation between $\theta_{10}(t)$ and $\theta_{N-10}(t)$ as a function of $A_{\rm left}$ and $A_{\rm f}$ with frozen solitons of width defined by (B) $W_{\rm f}$ and (C) $W^{\rm eff}_{\rm f}$.

find that the lower thresholds of the low cross-correlation region obtained considering a frozen perturbation or a right-initiated pulse follow similar trends (see Fig. 3B). However, there is a significant quantitative discrepancy between them that arises because the left-initiated soliton interacts for a time $\Delta t \propto (c_{\rm left} + c_{\rm right})^{-1}$ with the right-initiated pulse ($c_{\rm left}$ and $c_{\rm right}$ denoting the velocities of the left-initiated and right-initiated solitary waves before collision, respectively) and $\Delta t \propto c_{\rm left}^{-1}$ with the frozen perturbation. To overcome this difference, we equate the interaction times by shrinking the width of the frozen soliton according to

$$W^{\rm eff}_{\rm f} = \frac{c_{\rm left}}{c_{\rm right} + c_{\rm left}} W_{\rm f} \ , \qquad (6)$$

where $c_{\rm right}$ is given by Eq. (3) with $A = A_{\rm f}$. Remarkably, by replacing the width of the frozen solitons $W_{\rm f}$ with $W^{\rm eff}_{\rm f}$, we find that the boundaries of the low cross-correlation region match extremely well the thresholds $\mathcal{A}^{\rm left}_{\rm upper}$ and $\mathcal{A}^{\rm left}_{\rm lower}$ (see Fig. 3C). As such, our analysis reveals that the anomalous collisions observed in our system are a consequence of the soliton large-amplitude characteristics, which modify the properties of the underlying media. Specifically, the large rotations induced in the chain by a pulse enlarge the amplitude gap for solitons that excite rotations of opposite direction and this may block their propagation.

While in Figs. 1-3 we focus on the interaction between pulses initiated at the two ends of the chain, anomalous collisions can also be triggered when the solitons are sequentially excited at the same end. To demonstrate this, we numerically study the collision between two solitons with amplitude $A_{\rm left,1}$ and $A_{\rm left,2}$ initiated at the left end at time $t_1 = 0$ and $t_2 = 0.3$s, respectively. We find that if the two solitons excite rotations of the same sign and the second one is faster, the second pulse penetrates and overtakes the first one, and neither of them change their amplitude, shape or velocity (see Fig. 4A). By contrast, if the two solitons induce rotations of opposite sign, a single pulse emerges from the collision with the same direction as the first one, but with larger amplitude and, therefore, lower velocity (see Fig. 4B).

Having demonstrated that our system can support anomalous collisions that alter the characteristics of the interacting solitons, we now explore how these unusual effects can be exploited to actively manipulate and control the propagation of pulses. First, we note that anomalous collisions provide opportunities to remotely induce changes in the propagation velocity of a soliton, as they can either reverse (see Figs. 1H-I), increase (see Fig. 2D) or lower (see Fig. 4B) the pulses speed (see also Fig. S8A). Second, we find that anomalous collisions can be exploited to probe the direction of the rotations of a pulse by monitoring the "echo" of a probing soliton (see Figs. 4C and S8). Third, if the direction of rotations excited by the soliton is known, we can block its propagation by sending a sequence of relatively small pulses with opposite rotation direction (see Figs. 4D and S8).

To summarize, our experiments show that anomalous interactions can occur for vector elastic solitons supported by a mechanical metamaterial based on rigid rotating units. While two solitons that induce rotations of the same direction penetrate each other when they

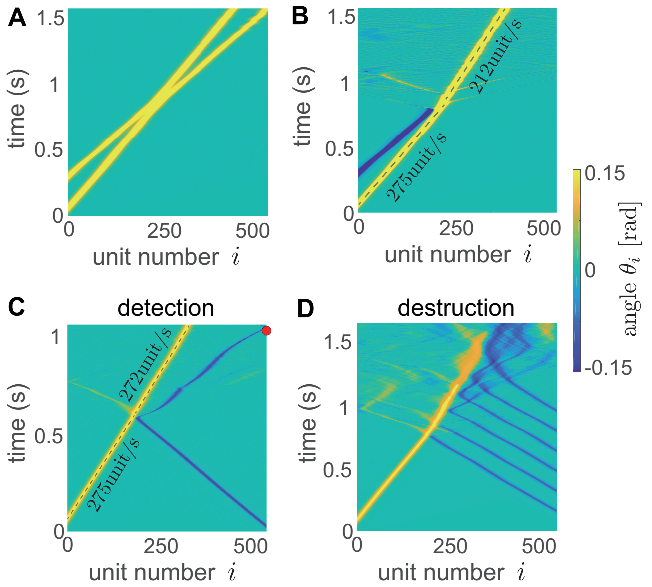

FIG. 4. (A)-(B) Rotations of the pairs of crosses as numerically found when considering two solitons of amplitude $A_{\text{left},1}$ and $A_{\text{left},2}$ ini tiated at the left end at time $t_1 = 0$ and $t_2 = 0.3$s. ($A_{\text{left},1}$, $A_{\text{left},2}$)=(0.4, 0.3) in (A) and (0.4, -0.3) in (B). (C) A soliton with amplitude $A_{\text{right}} = -0.18$ is excited from the right end as a probing soliton to detect the rotation direction of the main soliton of amplitude $A_{\text{left}} = 0.4$. (D) An amplitude $A_{\text{left}} = 0.4$ soliton is destroyed by six small solitons of amplitude $A_{\text{right},k} = -0.2$, (with $k = 1, ..., 6$).

meet, two solitons with opposite rotational component may repel each other and change both their amplitudes and velocities upon collision. Remarkably, our numerical analyses can fully explain the experimental findings and provide a complete description of these exotic two-soliton interactions. The geometric changes induced by one soliton significantly enlarge the effective amplitude gaps for other solitons with opposite rotational component and may block their propagation when they come close enough. We envision that the reported anomalous collisions between solitons could be used for remote control of the propagating nonlinear pulses, as they result in changes of the pulse velocity that can be engineered to remotely detect, change or destruct high-impact signals.

K. B. acknowledges support from the National Science Foundation under Grant No. DMR-1420570 and EFMA-1741685 and from the Army Research Office under Grant No. W911NF-17-1-0147

* bertoldi@seas.harvard.edu

[1] G. I. Stegeman and M. Segev, Science **286**, 1518 (1999).
[2] R. Radhakrishnan, M. Lakshmanan, and J. Hietarinta, Phys. Rev. E **56**, 2213 (1997).
[3] T. Tsuboi, Phys. Rev. A **40**, 2753 (1989).
[4] Y. Shen, P. G. Kevrekidis, S. Sen, and A. Hoffman, Phys. Rev. E **90**, 022905 (2014).
[5] H. K. Malik, R. Kumar, K. E. Lonngren, and Y. Nishida, Phys. Rev. E **92**, 063107 (2015).
[6] J. H. V. Nguyen, P. Dyke, D. Luo, B. A. Malomed, and R. G. Hulet, Nature Physics **10**, 918 (2014).
[7] J. Ibañez and E. Verdaguer, Phys. Rev. Lett. **51**, 1313 (1983).
[8] S. Sen, J. Hong, J. Bang, E. Avalos, and R. Doney, Physics Reports **462**, 21 (2008).
[9] F. Santibanez, R. Munoz, A. Caussarieu, S. Job, and F. Melo, Phys. Rev. E **84**, 026604 (2011).
[10] M. Manciu, S. Sen, and A. J. Hurd, Phys. Rev. E **63**, 016614 (2000).
[11] N. J. Zabusky and M. D. Kruskal, Phys. Rev. Lett. **15**, 240 (1965).
[12] P. Drazin and R. Johnson, Solitons: An Introduction, Cambridge Texts in Applied Mathematics (Cambridge University Press, 1989).
[13] T. Dauxois and M. Peyrard, Physics of Solitons (Cambridge University Press, 2006).
[14] V. G. Makhankov, Soliton Phenomenology (Kluwer Academic, 1989).
[15] B. Deng, J. Raney, V. Tournat, and K. Bertoldi, Physical Review Letters **118** (2017).
[16] B. Deng, P. Wang, Q. He, V. Tournat, and K. Bertoldi, Nature Communications **9**, 3410 (2018).
[17] B. Deng, V. Tournat, and K. Bertoldi, Phys. Rev. E **98**, 053001 (2018).
[18] C. Coulais, C. Kettenis, and M. van Hecke, Nature Physics , 1708.04643 (2017).
[19] A. Polyanin and V. Zaitsev, Handbook of Nonlinear Partial Differential Equations (Chapman and Hall/CRC, 2011).
[20] Y. S. Kivshar, J. Opt. Soc. Am. B **7**, 2204 (1990).
[21] M. Tabor, Chaos and integrability in nonlinear dynamics, Wiley-Interscience publication (Wiley, 1989).